

Comprehensive investigation on the aerodynamic behavior of transmission lines with distorted modeling

*Mu-Guang Liu¹⁾, Cheng Liu²⁾ and Zhuang-Ning Xie³⁾

^{1), 2), 3)} State Key Laboratory of Subtropical Building Science, SCUT, Guangzhou, China

ABSTRACT

The aerodynamic behavior of four-bundled transmission lines is examined through aeroelastic model based on distorted approach with a series of wind tunnel tests. Two distorted models and one normal model are simulated and tested for three kinds of uniform turbulent at wind yaw angles of 0°-45° with increments of 15°. The mean and RMS values of drag force and tension at each side of conductor as well as the PSD for the three models are obtained and discussed. The results indicate that turbulence and wind direction has a certain effect on the mean value and RMS value of the drag force and tension of the conductor, as well as the difference of force between the distorted model and normal model. For four-bundled conductor, it is recommended to use a horizontal distortion ratio around 0.8 instead of 0.5.

1 INTRODUCTION

Transmission lines systems are important lifeline product of the country. Due to the slenderness and flexibility of the system, it is vulnerable to strong wind loads. The transmission line system's response to wind load is nonlinear and complex due to the prominent movement of the lines under strong wind loads. The dynamic response of transmission tower is usually amplified by the wind-induced interaction between tower and transmission lines. Researchers attempt to reveal and conclude the dynamic rule of tower line system by field monitoring (Mehta Kishor and Kadaba, 1990; Momomura et al., 1997; Paluch et al., 2007; Takeuchi et al., 2010), numerical analysis (Yasui et al., 1999; Battista et al., 2003), and wind tunnel test (Huang et al., 2012; Liang et al., 2015; Hamada et al., 2017).

Compared with the other two research methods, wind tunnel testing is an attractive alternative. However, it is hard to accommodate several spans of tower line system in the wind tunnel due to the continuous long-span feature. Therefore, Loredou-Souza and Davenport (2001) proposed a novel approach for wind tunnel modelling of transmission lines and carried out a wind tunnel test on single conductors for investigating dynamic behavior of distorted model and normal model under strong wind. From the results obtained by them, it is apparent that the new modelling approach to conductor systems

¹⁾ Associate Professor

²⁾ Graduate Student

³⁾ Professor

in wind tunnels is a valid technique.

In this study, the aerodynamic behavior of four-bundled transmission lines is examined through aeroelastic model based on distorted approach with a series of wind tunnel tests. Two distorted models and one normal model are simulated and tested for three kinds of uniform turbulent at wind yaw angles of 0° - 45° with increments of 15° . The mean and RMS values of drag force and tension at each side of conductor as well as the PSD for the three models are obtained and discussed.

2 AEROELASTIC MODEL AND TESTING PROCEDURES

The prototype conductor adopted in the tests is JL1500 which is recommended in Chinese code of GB/T 1179-2008. As shown in Table 1, three conductor models with four-bundled type corresponding to the same prototype with a span of 125m were tested. Model M1 was a “normal” model which was designed and constructed at a geometric scale of 1:25 relative to the full-scale conductor. Model M2 and M3 were distorted model with the span correction coefficient $\gamma=0.8$ and 0.5 , respectively (Loredo-Souza and Davenport, 2001). Each conductor of the three four-bundled models consisted in using a copper cable to match the conductor axial stiffness, over which was the plastic hose to simulate the continuous external shape. In addition, lead wire was placed between the copper cable and plastic hose to match the mass per unit length.

Table 1 General characteristics of conductor prototype and models

Parameters	Span (m)	D* (mm)	Sag (m)	Mass* (kg/m)	f_1 (Hz)	Damping ratio (%)
Prototype	125	50.4	6.25	4.143	0.224	-
Scaling ratios	$\gamma:25$	$1:(25\gamma)$	1:25	$1:(25^2\gamma)$	5:1	1:1
M1(Normal)	5	2.05	0.25	0.0066	1.11	1.0
M2($\gamma=0.8$)	4	2.54	0.25	0.0083	1.18	1.1
M3($\gamma=0.5$)	2.5	4.08	0.25	0.0133	1.12	0.98

* represents the parameter of single conductor.

Two six-component high frequency force balances (HFFB), which the resolutions in x, y, and z axes are 0.005N, 0.005N, and 0.01N, respectively, were mounted at the two ends of conductor model and then fixed to a supporting system at 1m high, as shown in Fig.1. Four wind yaw angles, i.e. 0° , 15° , 30° and 45° , were tested. The definition of wind angle, β , is illustrated in Fig.2. The wind direction perpendicular to the conductor is defined as 0° . For each measurement, the effective sampling time was 120s with sampling frequency of 200 Hz after the wind field become stable.

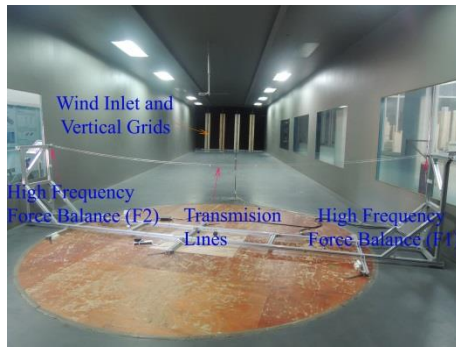


Fig. 1 Assembled aeroelastic transmission model

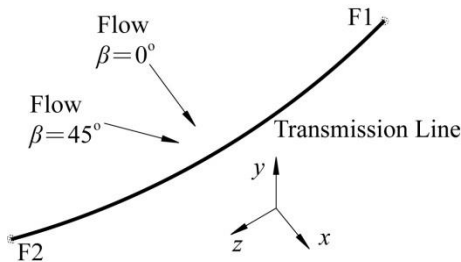


Fig. 2 Wind yaw angles and Coordinate System

Considering that the sag of the prototype transmission line is only 6.25m, the variation of wind speed and turbulence intensity along the height is very small. So three kind of uniform turbulent field are adopted in the tests, as shown in Fig.3. The turbulent field was simulated by properly vertical grids in the upstream of the wind tunnel section. The conductor model is located at the height of 75cm-100cm, and the turbulence intensity of the three wind fields in this range is around 3%, 9% and 13%, respectively. In addition, three kinds of wind speed from low to high were conducted to verify the stability of turbulent wind field. The three aeroelastic models were studied in the wind tunnel of South China University of technology, which is a closed jet return flow wind tunnel. M1 and M3 were conducted in the three turbulent fields, while M2 was only tested for low and medium turbulence fields.

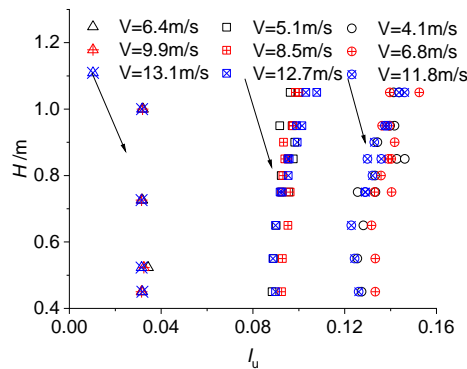


Fig. 3 Simulated wind parameters in wind tunnel

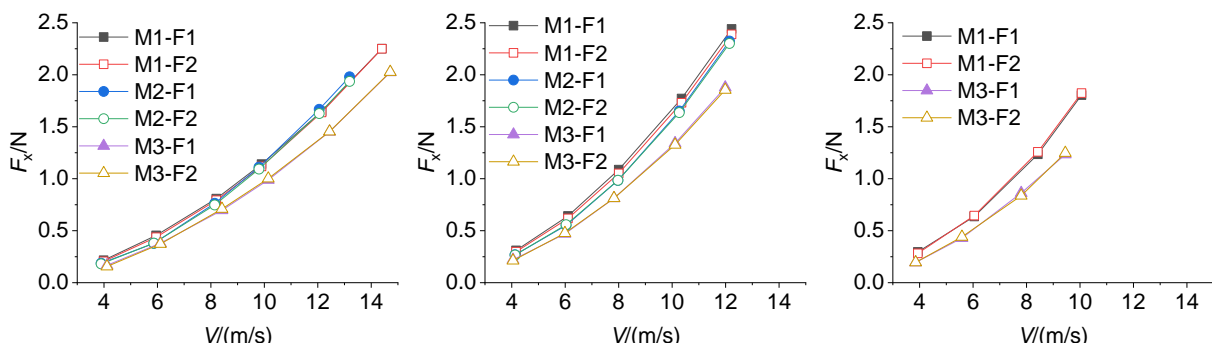
3 RESULTS AND DISCUSSION

3.1 Drag force

The relation between the drag force (F_x) mean values of the three conductors and wind speeds under $\beta=0^\circ$ at the three different turbulence fields is shown in Figs. 4. F1 and F2 in the figures represent the two ends of the model (the same below), the specific location is shown in Fig. 1 and Fig. 3. It can be seen from Fig. 4 that the drag force mean values of F1 and F2 at both ends of each model agree fairly well under different wind speeds, which further shows that the three uniform turbulent fields simulated in this paper have good spatial uniformity. With the increase of turbulence intensity, the mean values of the three models tend to increase at similar wind speed. The reason for that may be due to the fact that, the conductor is a flexible structure, and the local vibration of the conductor is obvious under the effect of turbulence, which leads to the enlargement of the local wake area of the conductor, thus increasing the drag force of the whole conductor.

According to Fig. 4 a), the mean values of M2 and M1 coincides very well in the test wind speed range under low turbulence intensity. At medium turbulence intensity, although the difference between M2 and M1 increases slightly, it still has good consistency. However, for M3, the values are generally lower than that of M1, and the difference tends to rise with the increase of wind speeds and turbulence intensity. Under the low wind speed of 4-6m/s at $lu=3\%$, there is little difference between M3 and M1, which is basically consistent with the conclusion obtained in Loredou-Souza and Davenport (2001) at 6 m/s wind speed.

The above results show that the mean drag force of the conductor will be reduced with the decrease of span under the same sag, which is mainly due to the weakening of the local micro vibration of the conductor. When the span is reduced by 20%, the reduction in mean drag force is not significant, but the span reduction of 50% will have a significant impact, which is acceptable only at low turbulence and low wind speed. What needs to be further explained is that, the results obtained by Loredou-Souza and Davenport (2001) shown that the mean values between the normal model and distorted model ($\gamma=0.5$) agree fairly well at medium and high turbulence intensity. The possible reasons are as follows: 1) a simplified lumped pieces is used by them to simulate the aerodynamic configuration, and the mean drag force amplification effect caused by local vibration of conductor is significantly weaker than that of the continuous aerodynamic shape simulated in this paper; 2) the research object they used is a single conductor, while the object in this paper is four-bundled conductors, which have certain aerodynamic interference.



sharing at the downstream. On the whole, the mean drag force at both ends of M2 in different wind directions is still consistent with that of M1, while there is still significant gap between M3 and M1 in oblique wind.

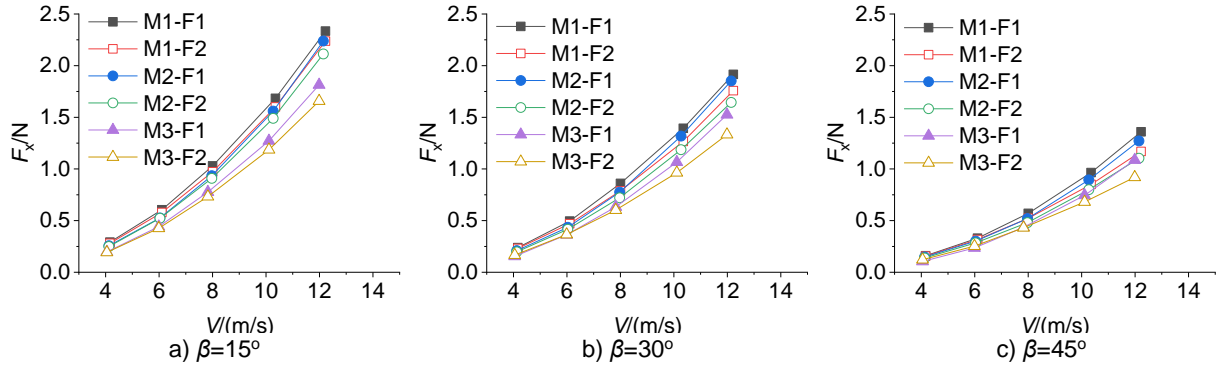


Fig. 6 Relation between drag force mean values and wind speeds for conductors at different directions ($I_u=9\%$)

Under the oblique wind, the drag force RMS values of F2 at the windward of conductor is smaller than that of F1 at the leeward, and the greater the wind direction, the more obvious the difference between them (Fig.7). The RMS values of F2 at upstream end of the three models are in good agreement, but there are still obvious differences in F1 at downstream end. For M2, the RMS value of F1 is still higher than that of M1 under different wind directions, but the difference between them gradually decreases with the increase of wind direction. For M3, the RMS value of F1 is slightly higher than that of M1 at the low wind speed of 4-8m/s, but at the high wind speed above 8m/s, the RMS value gradually changes from slightly higher than that of M1 to slightly lower than that of M1 with the increase of wind direction.

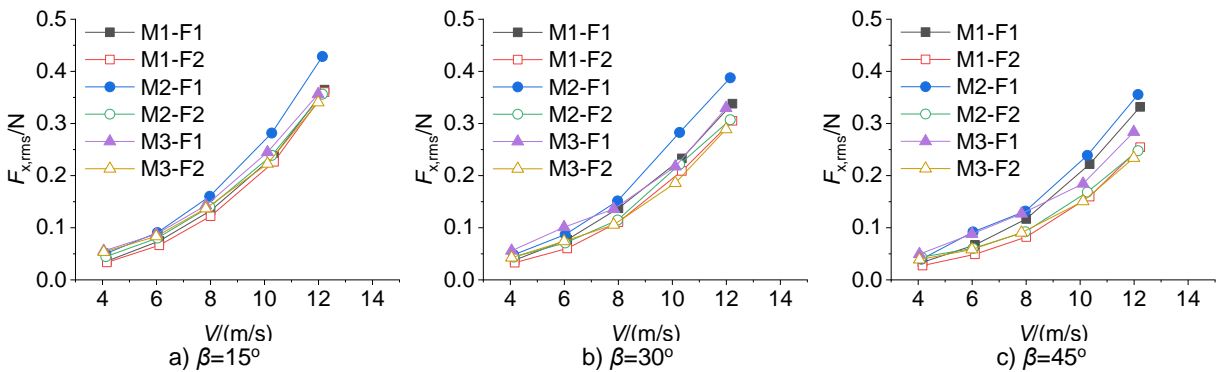


Fig. 7 Relation between drag force RMS values and wind speeds for conductors at different turbulence intensity ($I_u=9\%$)

3.2 Lift force

Due to the small lift magnitude, the regularity under different turbulence intensity level and wind directions is not significant. Only the relation of lift force with wind speed at $\beta=0^\circ$ under medium turbulence degree is presented in this paper, as shown in Fig.8. It can be seen that the mean lift force is about 1/8 of the mean value of drag force, and the RMS value is about 1/2 of that of drag force. The mean lift force of M2 is slightly lower than that of M1, and the trend of variation with wind speed is consistent with that

of M1, while the variation trend of M3 and M1 with wind speed is different, which only fits well at low wind speed of 4-6m/s. The RMS values of M2 and M3 have little difference, which are slightly higher than those of M1.

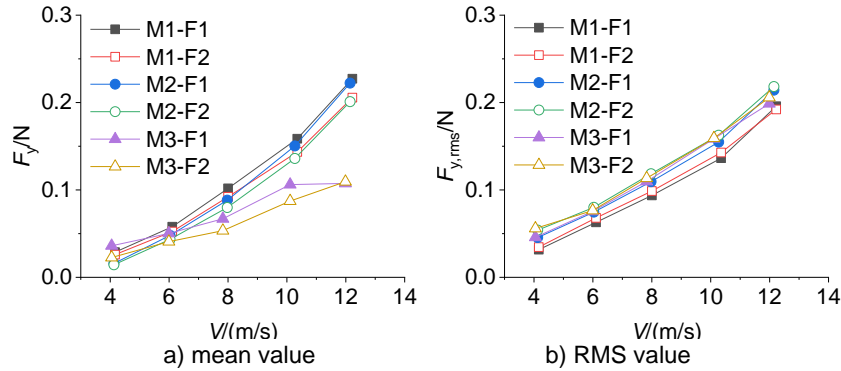


Fig. 8 Relation between lift force and wind speeds for conductors ($\beta=0^\circ$, $I_u=9\%$)

3.3 Tension

The relation between the mean tension (F_T) of the three conductors and wind speeds under $\beta=0^\circ$ at the three different turbulence fields is shown in Figs. 9. It can be seen that the mean tension of each model increases with the increase of turbulence intensity. For M2, the mean tension of M1 and M2 have excellent consistency at different wind speeds under low turbulence. Although the difference between them increases slightly in the medium turbulence intensity, it still has a good agreement. For M3, the mean tension at all three turbulence fields is great different from that of M1. This is because in the case of the same sag, the decrease of span will lead to the increase of the angle between the end of the line and the horizontal plane, resulting in the reduction of tension. It can be seen from the above analysis that 20% reduction of span has no significant effect on tension, but 50% reduction will have a significant impact.

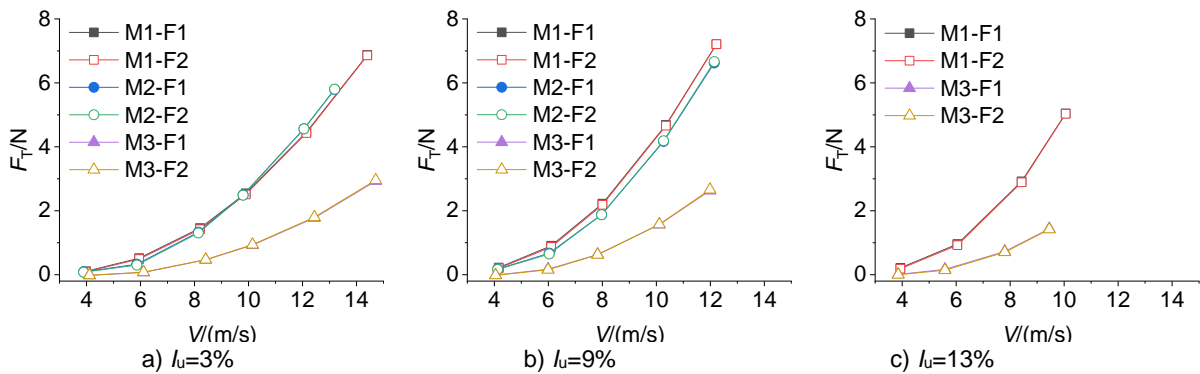


Fig. 9 Relation between mean tension and wind speeds for conductors at different turbulence intensity ($\beta=0^\circ$)

Fig. 10 shows the variation of tension RMS values of the three conductors with wind speeds under $\beta=0^\circ$ at the three different turbulence fields. The results indicate that the increase of turbulence intensity will lead to the increase of tension RMS values. For M2, the RMS values at both ends of M2 is higher than that of M1 under low and

medium turbulence intensity, and the difference between them increases with the increase of wind speed. However, with the increase of turbulence intensity, the difference in RMS values between M2 and M1 decreases slightly. For M3, the RMS value at low wind speed is consistent with that of M1, but with the increase of wind speed, the RMS value of M3 is significantly lower than that of M1, and the difference between them increases rapidly. As the turbulence intensity increases from 3% to 9%, the difference of RMS values between M3 and M1 increases obviously, and there is little change in the difference after further increasing the turbulence intensity to 13%.

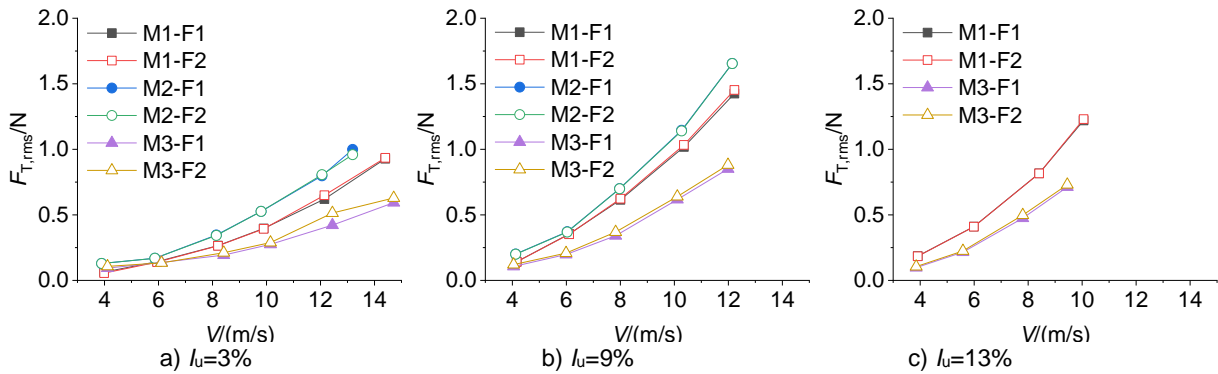


Fig. 10 Relation between tension RMS values and wind speeds for conductors at different turbulence intensity ($\beta=0^\circ$)

With the increase of wind direction, the mean tension at both ends of the conductor decreases gradually while the difference between them is increasing, and the mean tension of F2 is higher than that of F1 (Fig. 11). In addition, the difference of mean tension between the distorted model and normal model decreases slightly under skew wind. The RMS values at both ends of each model are basically the same under different direction, which is different from the law of drag and lift mentioned above. As wind direction increase, the difference of RMS between M2 and M1 decreases slightly, but the difference between M3 and M1 slightly increases somewhat.

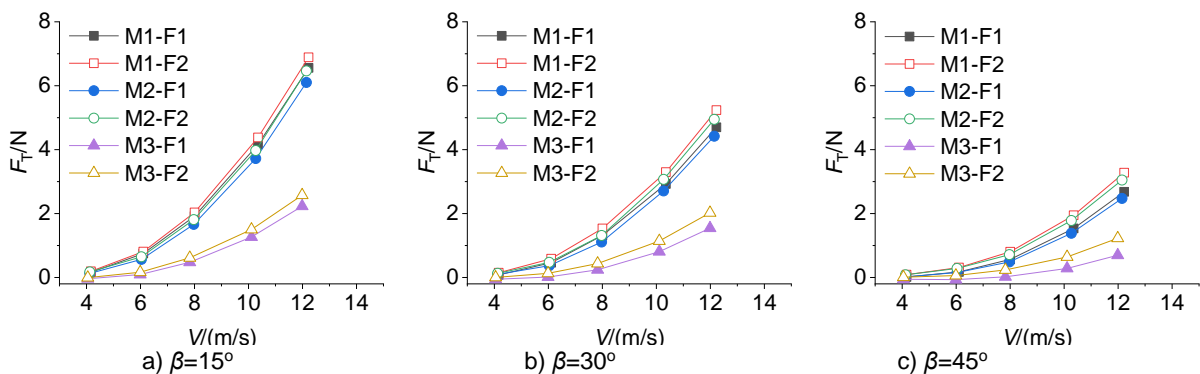


Fig. 11 Relation between mean tension and wind speeds for conductors at different directions ($I_u=9\%$)

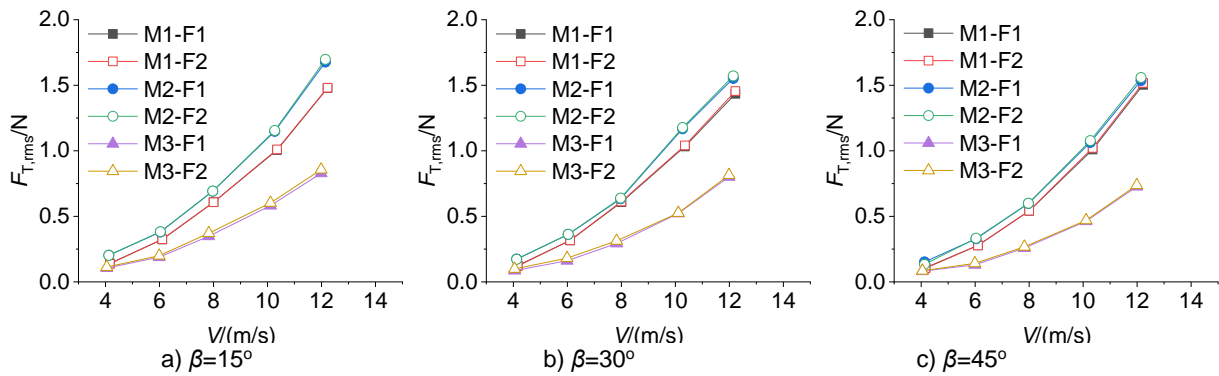


Fig. 12 Relation between tension RMS value and wind speeds for conductors at different directions ($I_u=9\%$)

3.4 Unbalance properties in F_x and F_T

Under oblique wind, there will be a certain difference between the drag and tension mean values at the two ends of the conductor, especially the difference in tension, which will cause the transmission tower to be pulled along the span wise. Fig. 13 shows the variation of drag force ratio and tension ratio (F_1/F_2) at both ends of the model with wind speed at medium turbulence. It can be seen that with the increase of wind direction, the non-uniformity of force at both ends of each model gradually increases, and the unbalance properties of tension is obviously higher than that of drag force. For M2, except for low wind speed, the F_1/F_2 ratios of drag force and tension have good consistency with that of M1. However, for M3, there is significantly different in unbalance properties of drag force and tension from that of M1.

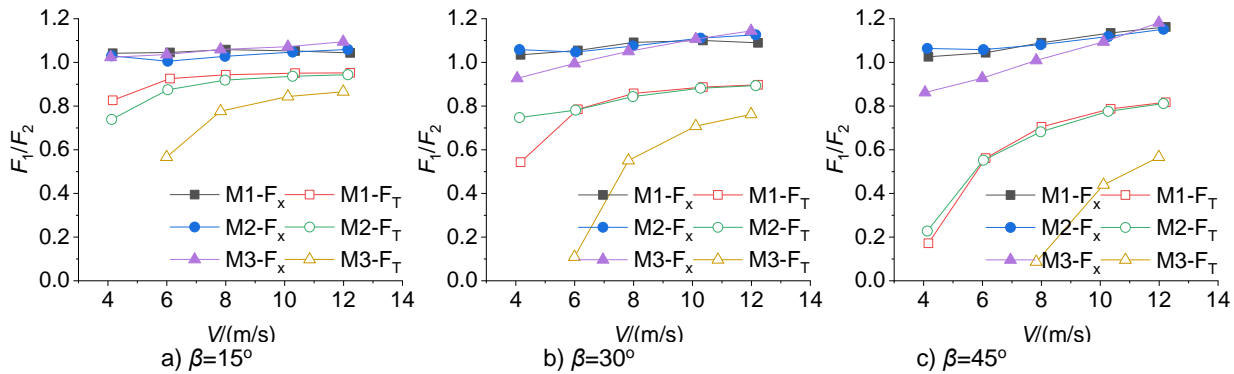


Fig. 13 Relation between unbalance forces and wind speeds for conductors at different directions ($I_u=9\%$)

3.5 Power spectrum density

Fig. 14 shows the power spectrum density (PSD) of drag forces and tensions at medium turbulence intensity. It can be seen that the drag force PSD of M1 has obvious peaks in the range of 2-3Hz and 5-10Hz, and there are also obvious peaks in the 3-5Hz and 7-10Hz of the tension PSD, which indicates that the higher-order modes of the conductor participate in the vibration. The PSD of drag force and tension for M2 keeps good consistency from that of M1 in the frequency range within 50 Hz. However, the PSD of M3 is consistent with that of M1 only at low frequency within 5Hz.

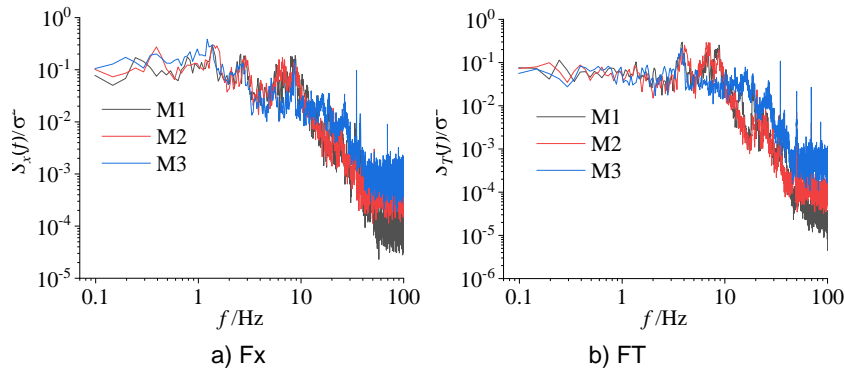


Fig. 14 PSD of drag force and tension at the end of F1 for the three conductors ($l_u=9\%$, $\beta=0^\circ$, $V=8\text{m/s}$)

4 CONCLUSIONS

1) For $\gamma=0.8$, the mean values of drag force and tension, and the non-uniformity of force at both ends of the distorted model are in good agreement with those of the normal model, but the RMS value is slightly higher than that of the normal model.

2) For $\gamma=0.5$, the mean values of drag force and tension, and the non-uniformity of force at both ends of the distorted model are different from those of the normal model. Meanwhile, the RMS values are slightly higher than that of the normal model, while the tension RMS values are lower than that of the normal model.

3) Turbulence has a positive effect on the mean value and RMS value of the conductor, and will increase the difference of mean value of drag force and tension as well as the drag force RMS value between the distorted model and the normal model. The influence on the tension RMS value is related to the horizontal distortion ratio γ .

4) The yaw wind will increase the non-uniformity of the force at both ends of the conductor, but will reduce the difference of mean value and RMS value between the distorted model and the normal model.

5) For four-bundled conductor, it is recommended to use a horizontal distortion ratio around 0.8 instead of 0.5.

Acknowledgements

The research described in this paper was financial supported by the National Science Foundation of China (51978285), the Fundamental Research Funds for the Central Universities (2015ZZ018), and National Engineering Laboratory for High Speed Railway Construction (2017HSR06).

REFERENCES

- Battista, R.C., Rodrigues, R.S., Pfeil, M.S. (2003), "Dynamic behavior and stability of transmission line towers under wind forces. " J. Wind. Eng. Ind. Aerod. Vol. 91 (8), 1051–1067.
- GB/T 1179-2008, (2009). "Round Wire Concentric Lay Overhead Electrical Stranded Conductors." Standards Press of China, Beijing (in Chinese).

- Hamada, A., King, J. P. C., El Damatty, A. A., Bitsuamlak, G., and Hamada, M. (2017), "The response of a guyed transmission line system to boundary layer wind." *Engineering Structures*, Vol. 139, 135-152.
- Huang, M.F., Lou, W.J., Yang, L., et al. (2012), "Experimental and computational simulation for wind effects on the Zhoushan transmission towers. " *Struct. Infrastruct. E.* 8 (8), 781–799.
- Liang, S.G., Zou, L.H., Wang, D.H., et al. (2015), "Investigation on wind tunnel tests of a full aeroelastic model of electrical transmission tower-line system. " *Eng. Struct.* 85, 63–72.
- Loredo-Souza, A. M., and Davenport, A. G. (2001), "A novel approach for wind tunnel modelling of transmission lines." *Journal of Wind Engineering and Industrial Aerodynamics*, Vol. 89(1), 1017-1029.
- Mehta Kishor, C., and Kadaba, R. (1990), "Field data analysis of electrical conductor response towinds. " *J. Wind. Eng. Ind. Aerod*, Vol. 36 (1), 329–338.
- Momomura, Y., Marukawa, H., Okamura, T., et al. (1997), "Full-scale measurements of wind-induced vibration of a transmission line system in a mountainous area. " *J. Wind. Eng. Ind. Aerod*, Vol. 72, 241–252.
- Paluch, M.J., Cappellari, T.T.O., Riera, J.D. (2007), "Experimental and numerical assessment of EPS wind action on long span transmission line conductors. " *J. Wind. Eng. Ind. Aerod*, Vol. 95 (7), 473–492.
- Takeuchi, M., Maeda, J., Ishida, N. (2010), "Aerodynamic damping properties of two transmission towers estimated by combining several identification methods. " *J. Wind. Eng. Ind. Aerod*, Vol. 98 (12), 872–880.
- Xie, Qiang, Cai, Yunzhu, and Xue, Songtao. (2017), "Wind-induced vibration of UHV transmission tower line system: Wind tunnel test on aero-elastic model." *Journal of Wind Engineering and Industrial Aerodynamics*, Vol. 171(1), 219-229.
- Yasui, H., Marukawa, H., Mommura, Y., et al. (1999), "Analytical study on wind-induced vibration of power transmission towers. " *J. Wind. Eng. Ind. Aerod.* 83 (1–3), Vol. 431–441.